Title
Multimodal imaging guidance for laser ablation in tracheal stenosis

Journal
The Laryngoscope, 120(9)

ISSN
0023-852X

Authors
Murgu, Septimiu D
Colt, Henri G
Mukai, David
et al.

Publication Date
2010-09-01

DOI
10.1002/lary.21047

Published in final edited form as:
Laryngoscope. 2010 September ; 120(9): 1840–1846. doi:10.1002/lary.21047.

Multimodal Imaging Guidance for Laser Ablation in Tracheal Stenosis

Septimiu D. Murgu, MD, **Henri G. Colt, MD**, **David Mukai, PhD**, and **Matt Brenner, MD**
Pulmonary and Critical Care Medicine (S.D.M., H.G.C., M.B.) Department of Medicine, University of California School of Medicine, Irvine, California, U.S.A and Beckman Laser Institute (D.M., M.B.), University of California, Irvine, Irvine, California, U.S.A

Abstract

Objective/Hypothesis—Laser-induced damage of tracheal wall microstructures might contribute to recurrence after bronchoscopic treatment of tracheal strictures. The purpose of this study was to demonstrate how multimodal imaging using white light bronchoscopy (WLB), endobronchial ultrasound (EBUS), and optical coherence tomography (OCT) might identify in vivo airway wall changes before and resulting from Nd:YAG laser ablation and dilation of tracheal stenosis.

Study Design—Case study.

Methods—Commercially available WLB, high frequency EBUS using a 20-MHz radial probe and time-domain, frontal imaging OCT systems were used to characterize the extent, morphology, and airway wall microstructures at the area of hypertrophic fibrotic tissue formation before, during and after treatment of postintubation tracheal stenosis.

Results—WLB revealed the location of a complex, extensive, severe stricture. EBUS showed a homogeneous layer overlying a hyperechogenic layer corresponding to disrupted cartilage. OCT showed a homogeneous light backscattering layer and absence of layered microstructures, confirming absence in close proximity of normal airway wall. After laser ablation, OCT of charred tissue showed high backscattering and shadowing artifacts. OCT of noncharred tissue showed a thinner, homogeneous, light backscattering layer. EBUS showed thinner but persistent hypertrophic tissue suggesting incomplete treatment. WLB revealed improved airway patency postprocedure and recurrence 3 weeks later.

Conclusions—EBUS identified cartilage disruption and residual hypertrophic tissue, the evidence of which might contribute to recurrence. OCT revealed homogeneous light backscaterring representing persistent noncharred hypertrophic tissues but it did not visualize cartilage disruption. Future studies are warranted to confirm whether these technologies can help guide bronchoscopic treatments.

Send correspondence to Dr. Septimiu D. Murgu, UCI Medical Center, 101 the City Drive South, City Tower, Suite 400, ZOT code 4095, Orange, CA 92868-3217. smurgu@uci.edu.

The authors have no financial disclosures and no conflicts of interest related to the content of this article.

Keywords

Multimodal imaging; bronchoscopy; optical coherence tomography; endobronchial ultrasound; tracheal stenosis

Introduction

Bronchoscopic treatment of complex postintubation tracheal stenosis is offered when open surgical resection is not indicated either because of stricture length, severe comorbidities, desire to attempt minimally invasive treatments, or when impending death warrants urgent restoration of airway patency.[1] Stricture recurrence after bronchoscopic treatment is frequent, suggesting that the nature of the treatment itself, which often includes laser resection and mechanical dilation, might induce or exacerbate airway wall injury.[1] Histologic examination of excised specimens has confirmed that mucosal and submucosal hypertrophy accompanied by exuberant fibrosis, and, at later stages, fragmentation of cartilage and replacement by fibrotic tissue, characterizes complex strictures.[2,3] Results from experimental studies in canine tracheas also demonstrate how cartilage injury might cause tracheal stenosis, and reveal the potential for laser-induced collateral damage to chondrocytes even at a distance from the laser induced mucosal lesion.[4]

Postintubation strictures usually result from an initial insult caused by the endotracheal tubes,[2] but may be exacerbated as a consequence of direct or collateral damage to the normal airway wall caused by the thermal effects of laser therapy during treatment.[4] Laser-induced tissue effects are determined by laser wavelength, power density, tissue color, and absorption coefficients. The potential for collateral damage of surrounding tissues warrants appropriate control of laser–tissue interactions, much of which currently depends on subjective visual and tactile feedback from the surface ablation site.[5]

Effective management of tracheal stenosis requires an assessment of the etiology, morphology of the stricture, determination of the extent of resection, and circumference of dilation, precise intraoperative technique, and an estimation of the risk for recurrence.[1] Until recently, there has not been a way to accurately assess, from an imaging perspective, each of these components in a comprehensive, objective fashion. Computed tomography with three-dimensional spatial reconstruction and new bronchoscopic technologies, however, now provide capabilities that may allow for a more accurate assessment of airway wall structure and characterization of the stricture before, during, and after treatment. The purpose of this study, therefore, was to demonstrate the feasibility of using a multimodal imaging platform including novel acoustic and optical bronchoscopic technologies to complement traditional diagnostic studies in order to: 1) identify in vivo airway wall changes before and resulting from Nd:YAG laser ablation and dilation, and 2) determine whether such real-time assessments might have a role in guiding bronchoscopic treatment.

Methods

A patient with a history of previous intubation for nonpenetrating trauma after a motor vehicle accident presented inextremis with stridor and shortness of breath at rest (WHO

functional class IV, MRC dyspnea scale 5). Flow volume loop showed fixed upper airway obstruction and severe reduction in forced expiratory flow. Flexible bronchoscopy revealed a complex, multilevel, hourglass stenosis 5 cm in length reducing airway lumen diameter to 6 mm at its most proximal portion, resulting in a stenosis index of 80% as calculated by morphometric bronchoscopy. Computed tomography of the neck and chest confirmed the hourglass-shaped stricture and suggested cartilaginous distortion (Fig. 1). The patient was studied at University of California, Irvine Medical Center in the operating room under rigid bronchoscopy with the technologies and equipment that follows. The study was approved by UC Irvine institutional review board (Protocol # 2006-4982).

A commercial two-dimensional, time-domain optical coherence front imaging tomography (OCT) system (Niris® Imaging system, Imalux® Corp, Cleveland, OH) and an endobronchial ultrasound (EBUS) system (Olympus Optical Co. Ltd, Tokyo, Japan) (Figs. 4 and 5) were used to further characterize the airway stricture and study airway wall microstructures in the region of hypertrophic fibrotic tissue comprising the stenosis. The OCT system has a depth resolution of 10–20 μm (in air), a lateral resolution of 25 μm, an imaging depth of ∼1.7 mm (in tissue), a lateral scanning range of 2 mm, a frame rate of 1.5 seconds/frame for 200 lateral pixel image, and a probe diameter of 2.7 mm. EBUS was performed using a 20-MHz radial mechanical-type ultrasonic probe (model UM-3R; Olympus) and an ultrasound unit (EU-M 20 Endoscopic Ultrasound System, Olympus) with resolutions that are typically no higher than 100 μm. Physical contact with the airway wall is achieved by using a water filled balloon to resolve transducer-tissue interface (Figs. 4 and 5).

Following completion of the initial studies including clinical examination, ventilatory function, computed tomography, and white light bronchoscopy (W.L.B.), the patient was taken to the operating suite for rigid bronchoscopy and Nd:YAG laser ablation and dilation (EFER rigid bronchoscope, Bryan Corp, Woburn MA; Laserscope, San Jose, CA, Nd:YAG 1064) to restore airway patency. Multimodality imaging studies including WLB, EBUS-radial probe, and OCT were repeated during and after the procedure to study the effects of resection on airway wall tissues.

The patient was intubated with a 12-mm diameter rigid bronchoscope under general anesthesia with spontaneous-assisted ventilation. With the rigid tube placed at the proximal aspect of the stricture, two radial incisions were made through the fibrotic tissue at the 9 o'clock (left anterolateral) and 5 o'clock (right posterolateral) positions using a bare fiber and near-contact mode (high power density with laser settings of 1 second, 30 W, pulsed mode). Total energy delivered was 2,538 Joules. Inspired oxygen fraction was kept at less than 0.4 during laser application. The stenotic area was then progressively dilated using the rigid scope. Residual tissues were removed by cup forceps taking care to avoid tearing tissues from normal airway wall.

Results

WLB showed no mucosal changes that would be suggestive of other airway disorders such as Wegener's granulomatosis, amyloidosis, tuberculosis or *Klebsiella rhinoscleromata*. The

stenosis itself was complex, multilevel, and circumferential in morphology, with an extent of 5 cm and with a stenotic index of 80%. Mucosa was slightly erythematous and edematous prior to resection. The right postero-lateral (5 o'clock position) and the left anterolateral hypertrophic tissues were noted to be firm on palpation with the rigid suction catheter (Fig. 1). EBUS-radial probe imaging of these hypertrophic tissues revealed an isoechoic homogeneous layer overlying a hyperechogenic layer corresponding to tracheal cartilage. There was evidence of cartilage disruption at the proximal level of the stricture (Figs. 4 and 5). At this level a brighter echogenicity of cartilage was seen compared to normal cartilage, suggesting calcification (Fig. 5). In vivo OCT imaging of hypertrophic tissues showed a “bland” image consisting of homogeneous light backscattering and absence of layered microstructure, confirming the absence in close proximity of normal airway wall, which would be characterized by ordered layered microstructures (Figs. 2 and 3).

After radial incision and dilation, WLB revealed improved airway patency. EBUS-radial probe showed a reduction in the thickness of hypertrophic tissue at both the right and the left-sided treatment sites (Figs. 4 and 5). OCT imaging of charred fibrotic tissue showed high backscattering, reduced imaging penetration, and shadowing artifacts identified as vertical low backscattering streaks (Fig. 2). OCT imaging in areas without laser-induced charring, on the other hand, showed thinned hypertrophic tissues and a “bland” pattern similar to pretreatment image, confirming the continued absence of normal airway wall proximity (Fig. 3).

The patient was extubated and discharged the following day. Subsequent computed tomography, pulmonary function, and clinical assessments revealed symptomatic improvement, improved airway lumen diameter, normalization of the inspiratory limb with improvement of the expiratory curve, and improved functional class to WHO I. Three weeks later, however, new onset of exertional dyspnea (WHO class III, MRC scale 3) prompted WLB, which showed that the stricture had recurred (Fig. 1).

Discussion

The results from this study show how the addition of radial probe EBUS and OCT to standard WLB might help identify in vivo real-time changes in airway wall structures and hypertrophic stenotic tissues. The findings from multimodality imaging could potentially assist operators plan and proceed with ablation and dilation while maintaining an accurate and objective, rather than a visually subjective assessment of the extent of hypertrophic tissue removal, collateral damage to airway mucosa, and integrity of airway cartilage.

It is well known that subepithelial tissues play a leading role in the origin of tracheal stenosis, and that strictures can be caused by nonphysiological mechanical or thermal injuries,[6] which may, in part, explain the high recurrence rate after bronchoscopic laser therapy. Experimental studies in canines have shown that Nd:YAG laser-induced injury produced by a 50-J intensity beam is confined to the mucosa and submucosa, with no destruction of tracheal cartilage. This intact mucosa at the stenotic site may serve as a platform for normal reepithelialization and airway repair,[7] minimizing hypertrophic fibrotic tissue formation responsible for stricture recurrence. Greater energy delivery can destroy

airway wall structures, and strong correlations have been demonstrated between laser intensity, magnitude of tracheal injury, and collateral damage, especially when the laser is directed perpendicularly toward the airway wall.

In addition, destruction of normal airway wall mucosa around the stenotic area may predispose to disorganized healing by second intention, excessive fibrous tissue formation, and consequent stricture recurrence.[7] Laser-induced vaporization in proximity to cartilaginous structures can expose denuded cartilage, weaken the laryngotracheal framework, and induce restenosis to a more severe grade.[8] Variable tissue absorption of laser energy is typical, and is a function of the physical and chemical composition of the absorbing medium. However, deep tissue penetration often occurs with little evidence of superficial tissue damage, making laser effects in the airway difficult to assess. Because the thermal effects of Nd:YAG laser are, in part, characterized by wide scatter into adjacent tissues, shallow depth of penetration can still damage cartilage, especially if the laser fiber is not perfectly parallel to the airway wall[7] and a noncontact mode is used.[9]

The risk for recurrence after laser ablation and dilation of complex postintubation tracheal strictures, estimated to be greater than 70%, appears to be higher than that of simple web-like stenoses.[1,7] CT is a useful diagnostic modality for characterizing aspects of the stricture, revealing extrinsic compression when present, and identifying increased width of endoluminal soft tissues of the trachea as the principal cause of tracheal narrowing. However, supplemental tests such as paired inspiratory–expiratory dynamic CT or multiplanar reformatting are necessary to evaluate potential expiratory central airway collapse, allow accurate measurements of the stenotic area and delimit proximal and distal airway segments. CT scan resolution varies between 500 μm and 1 mm, which is insufficient to identify tissue microstructure. Furthermore, the needed high-speed intraoperative CT guidance is currently limited by size, cost, and complexity.[5]

WLB examination allows operators to precisely localize airway narrowing, estimate degree of severity, measure vertical extent and the numbers of rings involved, describe morphology, assess vocal cord and laryngeal function, determine presence of mucosal inflammation, and visualize mucosal changes suggestive of etiologies that might affect management decisions. But WLB provides little or no information regarding airway wall microstructure, and the assessment of collateral damage and proximity/integrity of airway cartilage before or after treatment is mostly subjective.

Investigators have used acoustic imaging technologies, such as radial probe EBUS to identify normal airway wall layers and cartilaginous disruption in tuberculosis, cancer, or malacia due to chronic inflammation, relapsing polychondritis and vascular abnormalities.[10] The results of our study suggest that radial probe EBUS might also be used to identify hypertrophic tissues and the integrity/proximity of airway wall cartilaginous layer before, during, and after bronchoscopic laser ablation and dilation of a tracheal stricture.

On excised specimens, exuberant fibrosis is seen, and light microscopy examination of paraffin sections reveal hypertrophy of the mucosal and submucosal layers of the stenotic segment.[2] Individual cartilage rings are often difficult to identify because of fibrotic

transformation of the trachea associated with chronic inflammation. Contrary to cases of idiopathic tracheal stenosis in which cartilage is relatively normal with a smooth inner and outer perichondrium, chondritis in patients with postintubation strictures is usually accompanied by extensive degeneration of cartilage with irregular borders of inner perichondrium.[2,3] In one histopathology study, for example, necrosis with regional loss of cartilage, extensive loss of cartilage, or complete replacement by hypertrophic fibrotic tissue was seen in 79% of patients while ossification of cartilage was present in 68%.[3] Focal ossification, similar to that observed sonographically in our case, was seen in 8% of patients.

In many cases, especially when there is cartilage degeneration or fragmentation, the expansile force of remaining cartilage is weaker than the strength of fibrotic contracture.[11] In addition, residual hypertrophic tissue after bronchoscopic resection and dilation probably contributes to this imbalance. Surgical data have shown that incompletely excised fibrous tissue is a major risk factor for recurrence after open resection of postintubation strictures.[12] Radial incisions performed as part of bronchoscopic laser ablation release the tension in the stricture prior to mechanical dilation, yet the majority of patients recur. This suggests that incomplete radial incisions, collateral airway mucosal damage, and denuded or fragmented cartilage resulting from the treatment itself also contribute to increased risk for recurrence. Therefore, the EBUS evidence of cartilaginous wall disruption at the proximal level of the stricture and the residual hypertrophic tissue identified in this study might be predictive factors for recurrence after laser ablation and dilation.

The pathologic effects of laser-induced hyperthermia within biologic tissues, although well characterized in histologic specimens, are ascertained only indirectly in vivo by observing superficial tissue blanching or charring during white light bronchoscopy. Experimental ex vivo studies of nonpulmonary tissues, however, have shown that OCT is able to detect dynamic changes induced by surgical laser ablation and to monitor tissue response during laser ablation.[5] Because the thermal injury disrupts the normal optical properties of the tissue, OCT can potentially more accurately monitor distributions of ablative damage.[5]

In our study we demonstrate how OCT can be used during bronchoscopic treatment of a tracheal stricture to identify hypertrophic tissues and normal layered micro-structures of the airway wall. Hypertrophic tissue presents as a “bland” image characterized by lack of layered microstructures of the normal airway wall (Figs. 2 and 3). As the ordered multilayered anatomy of the healthy airway is disrupted by structural remodeling consequent to the development of inflammation, OCT tomograms reflect “bland” images that ignore the boundaries of normal microstructures.[13]

Inflammation is characterized by a loss visualization depth below the epithelial and lamina propria layers on OCT imaging. This appears to result in part from the presence of infiltrating inflammatory cells that have a high nuclear density, modulating the refractive index of the imaged bulk tissue.[13] This might explain the highly backscaterring layer seen on the OCT images of the charred fibrotic tissue occurring as a result of laser-induced carbonization in our patient. The OCT findings in charred tissue are consistent with previous ex vivo studies showing shadowing artifacts identified by vertical low backscattering streaks (Fig. 2).[5] High temperatures in the charred tissue create a carbonized layer at the tissue

surface that strongly absorbs and scatters both the incident Nd:YAG laser and OCT beams. Because of this, light penetration is reduced and shadowing artifacts appear, making further interpretation of OCT images impossible in this region. In the area without charring, on the other hand, penetration is not attenuated at the surface, and further interpretation is possible: the hypertrophic tissues were thinner after laser exposure and dilation, but the imaging pattern was unchanged and continued to show a “bland” OCT tomogram confirming the lack of normal airway wall proximity (Fig. 3).

Because of the limited imaging depth of 1.7 mm in tissues, the human tracheal cartilaginous wall was not completely visualized in cross section when using this OCT system. Although OCT detects the boundary between the submucosa and the inner portion of the cartilage, it did not detect cartilage injury, disruption, or fragmentation. In this regard, EBUS sufficed to detect cartilage disruption, and potentially predict recurrence at the time of this initial bronchoscopic evaluation.

In conclusion, the results from this study demonstrate that multimodality imaging including high-resolution, high-speed technologies such as OCT and radial probe EBUS are capable of imaging layered microstructures of the airway wall and visualizing the integrity or disruption of airway cartilage, respectively, in a patient with complex postintubation tracheal stenosis. Previous studies have shown that high-frequency EBUS identifies cartilage abnormalities in patients with tracheobronchomalacia[10] and accurately detects cartilaginous involvement in tumor invasion. Experimental studies of nonpulmonary tissues have shown that OCT is able to detect dynamic changes induced by surgical laser ablation,[5] although in vivo studies have shown that OCT can reveal airway wall microstructures in patients with both benign and malignant disease.[13–15]

Currently, the intraoperative assessments of the tissue effects of laser resection and dilation on airway strictures are usually subjective, based on visual and tactile feedback during WLB. The addition of acoustic and optical technologies such as OCT and radial probe EBUS provides capabilities for real-time, in vivo objective assessment of the effects of laser ablation and dilation on hypertrophic tissues and airway cartilage, respectively, in postintubation tracheal stenosis. Future studies are warranted to determine whether in vivo monitoring of these effects might help guide ablation, minimize collateral tissue damage, and decrease the risk of normal airway wall injury and subsequent recurrence of tracheal stenosis.

Acknowledgments

The work presented here was partially supported by grants from the National Institutes of Health (#CA 124967) and California TRDRP (16RT-0082).

Bibliography

1. Cavaliere S, Bezzi M, Toninelli C, Foccoli P. Management of post-intubation tracheal stenoses using the endoscopic approach. Monaldi Arch Chest Dis. 2007; 67:73–80. [PubMed: 17695689]
2. Cooper JD, Grillo HC. The evolution of tracheal injury due to ventilatory assistance through cuffed tubes: a pathologic study. Ann Surg. 1969; 162:334–348. [PubMed: 5266019]

3. Mark EJ, Meng F, Kradin RL, Mathisen DJ, Matsubara O. Idiopathic tracheal stenosis: a clinicopathologic study of 63 cases and comparison of the pathology with chondromalacia. Am J Surg Pathol. 2008; 32:1138–1143. [PubMed: 18545144]
4. Rebeiz EE, Aretz HT, Shapshay SM, Pankrotov MM. Application of pulsed and continuous wave 1.32 and 1.06 mm wavelengths of the Nd:YAG laser in the canine tracheobronchial tree: a comparative study. Lasers Surg Med. 1990; 10:501–509. [PubMed: 2263149]
5. Boppart SA, Herrmann J, Pitris C, Stamper DL, Brezinski ME, Fujimoto JG. High-resolution optical coherence tomography-guided laser ablation of surgical tissue. J Surg Res. 1999; 82:275–284. [PubMed: 10090840]
6. Minnigerode B, Richter HG. Pathophysiology of subglottic tracheal stenosis in childhood. Prog Pediatr Surg. 1987; 21:1–7. [PubMed: 3107065]
7. Mehta AC, Lee FYW, Cordasco EM, Kirby T, Eliachar I, DeBoer G. Concentric tracheal and subglottic stenosis: management using the Nd:YAG laser for mucosal sparing followed by a gentle dilatation. Chest. 1993; 104:673–677. [PubMed: 8365273]
8. Monnier P, George M, Monod ML, Lang F. The role of the CO2 laser in the management of laryngotracheal stenosis: a survey of 100 cases. Eur Arch Otorhinolaryngol. 2005; 262:602–608. [PubMed: 16021463]
9. Shapshay SM. Laser application in the trachea and bronchi: a comparative study of the soft tissue effects using contact and noncontact delivery systems. Laryngoscope. 1987; 97:1–26. [PubMed: 3110518]
10. Murgu S, Kurimoto N, Colt H. Endobronchial ultrasound morphology of expiratory central airway collapse. Respirology. 2008; 13:315–319. [PubMed: 18339038]
11. Jung Kwon O, Young Suh G, Pyo Chung M, Kim J, Han J, Kim H. Tracheal stenosis depends on the extent of cartilaginous injury in experimental canine model. Exp Lung Res. 2003; 29:329–338. [PubMed: 12888447]
12. Couraud L, Moreau JM, Velly JF. The growth of circumferential scars of the major airways from infancy to adulthood. Eur J Cardiothorac Surg. 1990; 4:521–525. [PubMed: 2245045]
13. Whiteman SC, Yang Y, Gey van Pittius D, Stephens M, Parmer J, Spiteri MA. Optical coherence tomography: real-time imaging of bronchial airways microstructure and detection of inflammatory/neoplastic morphologic changes. Clin Cancer Res. 2006; 12:813–818. [PubMed: 16467093]
14. Colt H, Murgu SD, Ahn YC, Brenner M. J Biomed Opt. 2009; 14:034035. [PubMed: 19566328]
15. Lam S, Standish B, Baldwin C, et al. In vivo optical coherence tomography imaging of preinvasive bronchial lesions. Clin Cancer Res. 2008; 14:2006–2011. [PubMed: 18381938]

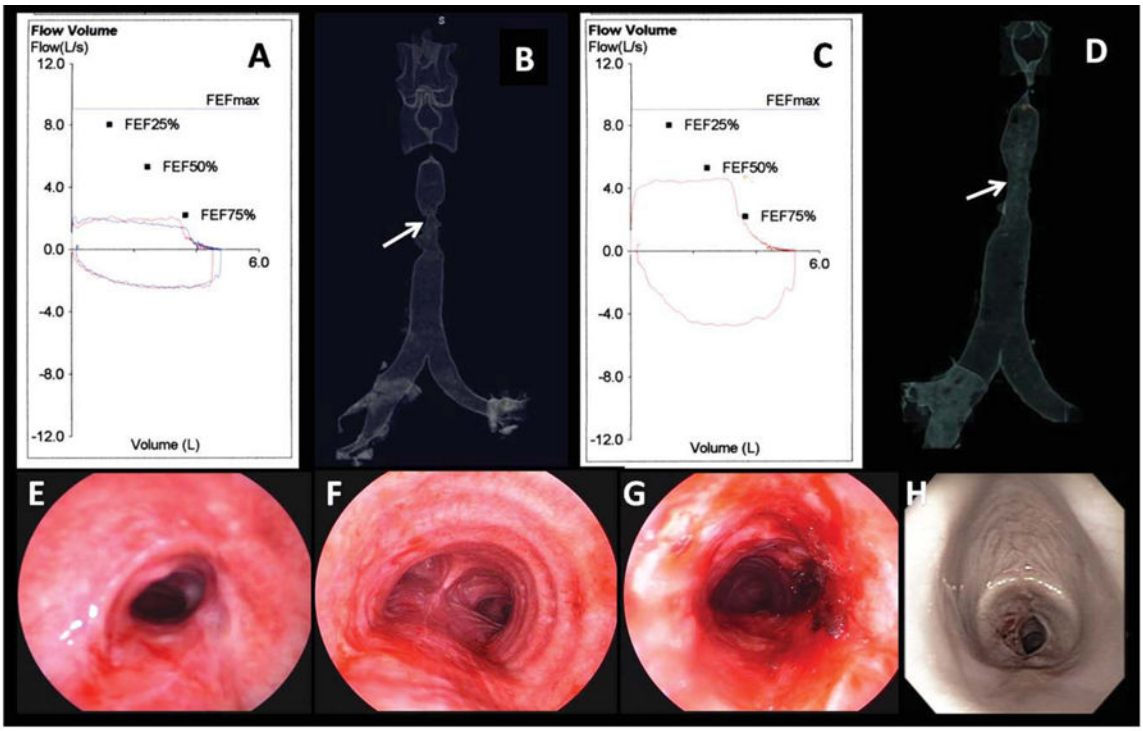

Fig. 1.

(**A**) FV loop preoperatively shows flattening of the inspiratory and expiratory loops characteristic of fixed upper airway obstruction. (**B**) 3D CT scanning tracheal surface rendering image revealed an “hourglass” complex, multilevel tracheal stenosis extending for 5 cm and of 6 mm diameter. (**C**) After laser and dilation, the FV loop and the inspiratory and expiratory flows have improved but not normalized. (**D**) 3D CT scanning postintervention showed no change in the morphology or extent of the lesion but improved airway diameter to 10 mm. (**E**) Bronchoscopic view of the proximal aspect of the stricture preoperatively showed severe degree of airway narrowing (SI = 80%). (**F**) Normal airway caliber distal to the stricture. (**G**) Proximal aspect of the stricture after laser and dilation showed improved patency (SI = 27%). (**H**) WLB shows recurrent severe (SI = 90%) stenosis at 3.5 cm below the vocal cords at 21 days postbronchoscopic treatment.

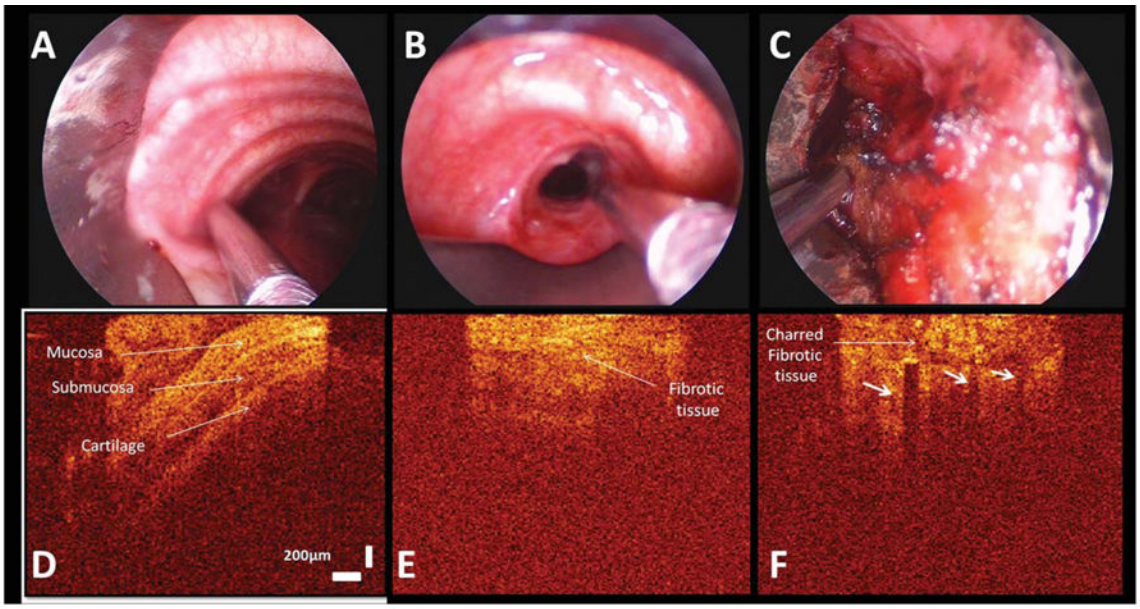

Fig. 2.

WLB image shows the OCT probe overlying the normal tracheal wall (**A**), the stricture at the right incision site before laser ablation (**B**), and after laser ablation on a area of charred fibrotic tissue (**C**). Two-dimensional OCT images reveal the normal airway wall structural layers (**D**). Mucosa provides enhanced reflectivity signals compared with adjacent surrounding submucosa. The extracellular matrix of cartilage decreases scattering of incident light and reflects as a dark region on the OCT image. OCT imaging of the right incision site before laser (**E**): the high thick backscattering area and resultant loss of layer structures is visible and likely explained by chronic inflammation, which disrupts tissue boundaries and shows a bland image that clearly lacks the ordered multilayered appearance of the healthy airway wall. OCT image of the charred fibrotic tissue after laser ablation (**F**): the high temperatures char tissue and create a carbonized layer at the surface, which rapidly absorbs and scatters the incident OCT imaging beam resulting in reduced OCT imaging penetration and causing shadowing artifacts, identified by vertical low backscattering streaks (arrows). The charred fibrotic tissue shows high backscattering after laser ablation. OCT image size is 2 mm horizontal and 2.2 mm (in air, vertical).

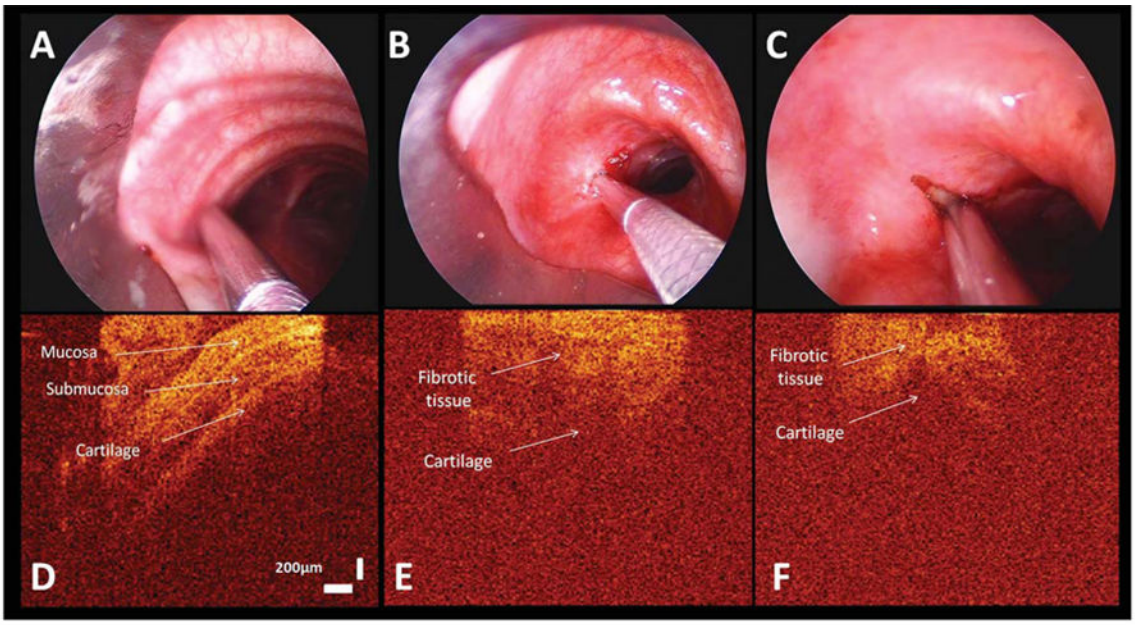

Fig. 3.

WLB image shows the OCT probe overlying the normal tracheal wall (**A**), the stricture at the left incision site before laser ablation (**B**), and after laser ablation on a area without charred fibrotic tissue (**C**). Two-dimensional OCT images reveal the normal airway wall structural layers (**D**). OCT image of the left incision site before laser shows similar findings as on the right side and reveals a bland image that lacks the ordered multilayered appearance of the healthy airway wall (**E**). OCT image of left incision site on an area without charred tissue after laser ablation (**F**). A thinner high backscattering layer of the residual fibrotic tissue and resultant loss of multilayered structure are identified. OCT image size is 2 mm horizontal and 2.2 mm (in air, vertical).

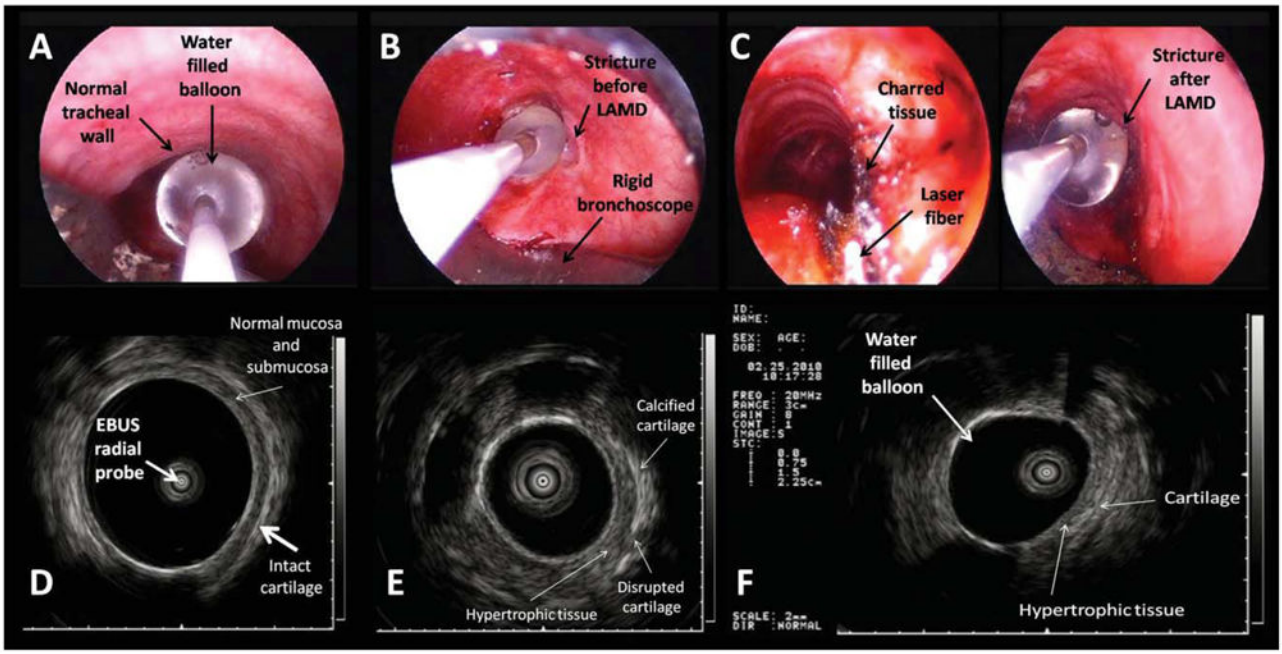

Fig. 4.

(**A**) WLB image shows the radial EBUS probe with the water-filled balloon overlying the normal tracheal wall. (**B**) The balloon completely occludes the airway lumen at the level of the stricture. (**C**) Close WLB view of the charred tissue, Nd:YAG laser fiber and water-filled balloon of the radial EBUS probe at the level of the right hypertrophic tissue. (**D**) EBUS image of the normal tracheal wall. The submucosa and the cartilaginous layers are clearly identified overlying the water-filled balloon used to resolve airway wall–transducer interface. (**E**) EBUS image of the stricture before laser at the level of the right hypertrophic tissue. The thick layer of the fibrotic, hypertrophic tissue is visualized overlying a portion of disrupted cartilage. The cartilaginous ring has a brighter echogenicity related to the normal airway cartilage suggesting calcification. (**F**) EBUS image of the stricture after laser and dilation shows thinner but residual right hypertrophic tissue.

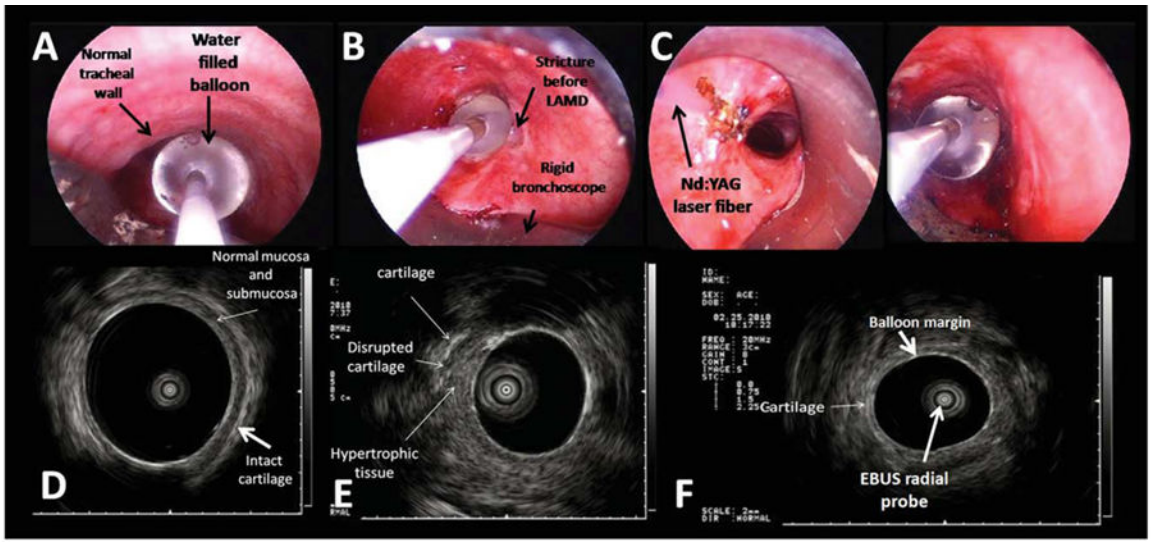

Fig. 5.

(**A**) WLB image shows the radial EBUS probe with the water-filled balloon overlying the normal tracheal wall. (**B**) The water-filled balloon completely occludes the airway lumen at the level of the stricture before laser and dilation. (**C**) WLB view of Nd:YAG laser fiber and water-filled balloon of the radial EBUS probe at the level of the left hypertrophic tissue. (**D**) EBUS image of the normal tracheal wall. The submucosa and the cartilaginous layers are clearly identified overlying the water-filled balloon. (**E**) EBUS image of the stricture before laser and dilation at the level of the left hypertrophic tissue. The thick layer of the hypertrophic tissue is visualized overlying a portion of disrupted cartilage. (**F**) EBUS image of the stricture after laser and dilation shows the water filled balloon overlying the cartilage.